

The Polyelectrolyte Nature of F-actin and the Mechanism of Actin Bundle Formation*

(Received for publication, November 10, 1995)

Jay X. Tang and Paul A. Janmey

From the Division of Experimental Medicine, Brigham and Women's Hospital, LMRC 301, Boston, Massachusetts 02115

Polymerized (F-)actin is induced to form bundles by a number of polycations including divalent metal ions, $\text{Co}(\text{NH}_3)_6^{3+}$, and basic polypeptides. The general features of bundle formation are largely independent of the specific structure of the bundling agent used. A threshold concentration of polycation is required to form lateral aggregates of actin filaments. The threshold concentration varies strongly with the valence of the cation and increases with the ionic strength of the solution. Poly-anions such as nucleoside phosphates or oligomers of acidic amino acids disaggregate actin bundles into single filaments. These features are similar to the phenomenon of DNA condensation and can be explained analogously by polyelectrolyte theories. Similar results were found when F-actin was bundled by the peptide corresponding to the actin binding site of myristoylated alanine-rich protein kinase C substrate protein (MARCKS) or by smooth muscle calponin, suggesting that a broad class of actin bundling factors may function in a common manner. Physiologic concentrations of both small ions and large proteins can induce actin interfilament association independent of a requirement for specific binding sites.

Actin polymerizes to double stranded filamentous form (F-actin) in solutions of physiological ionic strength (2 mM MgCl_2 and 100 mM KCl). At relatively high (>10 mM) concentrations of divalent cations such as Mg^{2+} , F-actin forms aggregates of various forms, characterized as types I, II, and III paracrystals (1). Stable Type III paracrystals appear as large and compact side-by-side aggregates, with additional morphological variations identified by analyzing electron micrographs (EM) (2–6). An EM specimen typically manifests several morphologies, for which no difference in experimental conditions can be assigned. The co-existence of these morphological states implies that the total free energies of the various bundle forms are similar, provided that an overall attractive interaction exists in order to bring the filaments together.

Chemicals that cause F-actin to form paracrystalline bundles, such as divalent cations at high concentrations (order of 10 mM) (4), trivalent cations (mM range) (7), and polyamines (3, 4) are similar to those which cause DNA condensation (8, 9), except that the latter effect requires consistently higher concentrations of polycations. Both effects also occur at low pH (<5.5), and at high osmotic pressure (by addition of polyethylene glycol, for example) (10). It is the goal of this paper to demonstrate that the mechanism of F-actin bundle formation is analogous to that established for DNA condensation.

The phenomenon of DNA condensation has been successfully treated by the theory of linear polyelectrolytes (11–14). A double stranded DNA at neutral pH has a linear charge spacing $b = 1.7 \text{ \AA}$, much less than the Bjerrum length, the distance between elementary charges at which the electrostatic interaction energy equals the thermal energy kT , i.e. $\lambda_B = e^2/4\pi\epsilon_0\epsilon kT$. In water, for example, the dielectric constant $\epsilon = 80$ at 20 °C and $\lambda_B = 7.1 \text{ \AA}$. According to the Manning counterion condensation theory (12), a consequence of DNA's high charge density is that a certain fraction of its charge is neutralized due to the territorial binding of counterions in the immediate environment (so-called condensed counterions which are free to diffuse along the polymer axis, but inhibited from diffusing away). The fraction of polyelectrolyte charge compensated by the condensed counterions is determined as the following equation,

$$\theta = \left(1 - \frac{1}{N\zeta}\right) \quad (\text{Eq. 1})$$

where N is the valence of the counterion and $\zeta = \lambda_B/b = 4.2$. In monovalent electrolytes, θ is calculated to be 76%. It may reach 88% in the presence of sufficient divalent cations. Hence the predicted delocalized binding is stronger for counterions of higher valence, in which case the charged polymer is neutralized to a higher degree.

The residual electrostatic repulsion between polyelectrolytes of like charge tends to keep them apart. This repulsive force decreases with the presence of polyvalent counterions, due to the enhanced charge condensation. In addition to the weakened electrostatic repulsion between charged polymers due to counterions, an attractive interaction can also be induced by two polymers sharing counterions. The fluctuation (15) and lateral redistribution (14) of counterions have each been shown theoretically to cause an attractive interaction between polyelectrolytes. At appropriate ionic conditions, a balance between attractive and repulsive forces occurs so that the filaments in suspension form aggregates. This aggregation may also involve other interactions such as hydration and van der Waals forces (11, 13). It has been estimated that DNA condensation occurs as θ reaches 90%, which requires a valence of 3 or higher.

Counterion condensation theory has been applied to other polyelectrolytes such as polystyrene sulfonate and heparinate (16, 17). Justification for applying this theory has come from several different treatments. For example, analytical solutions to the nonlinear Poisson-Boltzmann equation for a cylindrical polyelectrolyte (18, 19) provide a model generally consistent with that of the earlier counterion condensation theory. Similar predictions were also obtained by Monte Carlo simulations (20, 21). Alternatively, an interesting ligand binding model of counterion condensation was proposed (22), with an assumption analogous to the territorial binding in the Manning theory. In this paper, the simplified predictions from the original Manning theory are used to explain the phenomenon of bundle formation by F-actin. Different results and interpretations

* This work is supported by National Institutes of Health Grants AR38910 and HL19429. The costs of publication of this article were defrayed in part by the payment of page charges. This article must therefore be hereby marked "advertisement" in accordance with 18 U.S.C. Section 1734 solely to indicate this fact.

from alternative approaches have been discussed more recently (19, 23).

An actin filament has a lower linear charge density than DNA. Using the amino acid sequence of α -skeletal muscle actin, one residue of 3-methylhistidine, an acetylated N terminus and one molecule each of tightly bound divalent cation and ATP (24), each subunit of an actin filament bears 14 excess negative charges. In addition, roughly three histidines per monomer are likely to be protonated at pH 7.2. Based on 370 monomers per micron contour length, the linear charge density is approximately $4 e/nm$. This value has two implications: the average charge spacing along the filament axis is sufficiently small compared to the Bjerrum length to make the counterion condensation theory relevant ($\zeta = \lambda_B/b > 1$); but ζ is less than that of DNA, suggesting that a smaller percentage of charge needs to be neutralized for condensation to occur (Equation 1). Therefore, one expects actin bundles to form at similar, but consistently lower, concentrations of cations compared to DNA. This prediction is tested by analysis of the effects of a variety of inorganic and organic cations, including the actin binding domain of MARCKS¹ protein and the smooth muscle actin binding protein calponin.

MATERIALS AND METHODS

Proteins—Monomeric (G-)actin was prepared from an acetone powder of rabbit skeletal muscle according to Spudich and Watt (25). The nonpolymerizing solution contained 4 mM Hepes buffer at pH 7.2, 0.2 mM CaCl₂, 0.5 mM ATP, and 0.5 mM NaN₃. The buffer concentration was sufficient to ensure the stability of pH, since concentrated reagents were frequently added to actin samples. Actin was polymerized by 150 mM KCl, unless mentioned otherwise.

Human plasma gelsolin was purified by elution from DE52 ion exchange matrix in 30 mM NaCl, 3 mM CaCl₂, 25 mM Tris, pH 7.4, as described by Kurokawa *et al.* (26), rapidly frozen in liquid nitrogen and stored at -80°C .

Recombinant chicken gizzard α -calponin was produced as described in Gong *et al.* (51) and was a kind gift of T. Tao (27). The lyophilized powder was dissolved in 3 M KCl and dialyzed against 50 mM Hepes, 5 mM dithiothreitol, and 0.1 M KCl at pH 7.5. A concentrated stock solution of up to 100 μM was prepared, and the protein concentration was determined by spectrophotometry, assuming a specific absorbance of $0.74 (\text{mg/ml})^{-1} \text{cm}^{-1}$ at 280 nm.

Peptides—MARCKS peptide was purchased from Biomol, supplied as trifluoroacetate salt. A stock solution of 200 μM peptide was prepared in 50 mM Hepes at pH 7.5. Oligomers of arginine, lysine, histidine, and aspartic acid were synthesized and purified by Daina Biseniece, Ieva Liepkaula, and Ivars Lipsbergs at the Latvian Organic Synthesis Institute and were conveyed to us by Rolands Vegners. Polylysines of degree of polymerization larger than 10 were purchased from Sigma. All the other common chemicals are of research or analytical grade.

Measurements—90 degree light scattering measurements were performed using a Perkin-Elmer LS-5B luminescence spectrometer. Different settings of wavelength, slit combination, and sample cuvettes of several dimensions and geometries were explored to find experimental conditions with sufficient signal and minimal multiple scattering. The instrumental settings altered the magnitude of the signals but not the concentrations of cations at which scattering changes were evident. We initially chose 365 nm excitation and 375 nm emission to avoid reflective signals, and slit widths of either 3 nm (Figs. 1, 3, and 6) or 5 nm (Figs. 2, 7, and 8) for both beams. Another frequently used setting was 365 nm/370 nm wavelength and 3 nm/3 nm slit width (Figs. 4 and 5). High-UV transparent plastic cuvettes of 10×5 -mm inside dimensions were used for 600- μl samples of low actin concentrations (0.1–1.0 mg/ml). Smaller glass tubes of 6 mm diameter were used for more concentrated samples in order to avoid the saturation of light scattering signals (Fig. 3). Square cuvettes (10×10 mm) and a 1200- μl sample volume were used to generate the data of Fig. 6b. Polycations and nucleoside phosphates were prepared as stock solutions at neutral pH at least 20 times more concentrated than required in the final mixtures. Dilution effects which amounted to less than 5% were ignored.

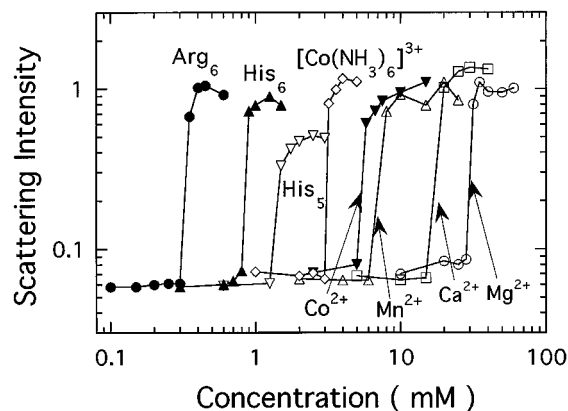


FIG. 1. Light scattering signal of F-actin as a function of concentration of various cations. Each sample contained initially 0.5 mg/ml F-actin at pH 7.2, followed by sequential additions of concentrated cations. The scattering was measured at 90 degrees, with 365 nm/370 nm wavelength and 3 nm/3 nm slit width (details under "Materials and Methods").

RESULTS

Bundle Formation by Metal Ions and Polyamines—The formation of F-actin bundles is conveniently detected by changes in light scattering. Fig. 1 shows the bundle formation of 0.5 mg/ml F-actin induced by a number of polycations. All the polyvalent cations were added in the form of concentrated chloride salts to ensure that the variation among these data was not attributable to anion species. The concentration of cations needed for the onset of bundling increases with decreased valence, indicating weakening ability to bundle. Hexamers of arginine bundle more efficiently than those of histidine, apparently because they carry a higher amount of net positive charges. D- and L-lysine isomers had identical effects (data not shown). The minimal bundling concentration of lysine hexamers (not shown) is almost the same as that of the arginine, indicating equally complete titration of one amine per side chain at pH 7.2. An intriguing result is that oligohistidines are fairly efficient actin bundlers at neutral pH, although the pK value for its side chain amine is as low as 6.5 and hence most of the side chains should be neutral. These oligomers of histidine either have more specific binding to F-actin or else they form small aggregates capable of bundling actin.

In order to confirm that an increase in light scattering corresponds to bundling, F-actin samples at different light scattering levels due to additions of polycations were examined by electron microscopy (EM), using the negative staining technique. When light scattering signals remained at low levels, actin filaments appeared disperse or intertwined in loose isotropic networks. In contrast, large lateral aggregates were always seen by EM at high light scattering levels.

The bundling efficiency of different divalent metal ions increases with their atomic number. Co²⁺ bundles F-actin at 5.5 mM, Mn²⁺ at 7 mM, in comparison with Ca²⁺ at 20 mM and Mg²⁺ at 27 mM. This variation from 5.5 to 27 mM may correlate with ionic radius and extent of hydration. Such cation-specific effects cannot be explained by the Manning theory.

The general behavior shown in Fig. 1 can be qualitatively explained by the predictions of the polyelectrolyte theory. Assuming an average linear charge density of $4 e/nm$ and applying the counterion condensation theory of Manning, a layer of condensed counterions is predicted near the F-actin surface. With 150 mM KCl and no polyvalent cations, the most simplified Manning model estimates K⁺ in this layer to be about 60% (Equation 1) of the total net surface charge of F-actin. If divalent cations are abundant in solution, the

¹ The abbreviation used is: MARCKS, myristoylated alanine-rich protein kinase C substrate.

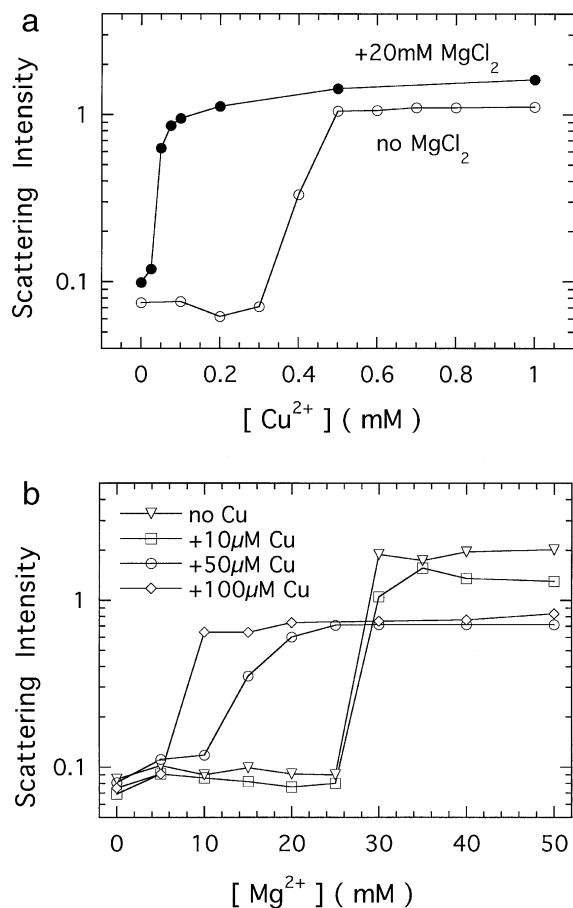


FIG. 2. Bundle formation of 0.2 mg/ml F-actin in 150 mM KCl, plus Cu^{2+} and/or Mg^{2+} . *a*, Cu^{2+} was sequentially added to F-actin solution, without (open circles) and with (solid circles) 20 mM MgCl_2 . *b*, MgCl_2 induced bundle formation of F-actin which was preincubated for roughly 5 min with 0, 10, 50, and 100 μM CuCl_2 .

percentage is estimated to be 82% (Equation 1). F-actin forms stable bundles at 150 mM KCl with order of 10 mM divalent cations, suggesting that approximately 80% neutralization of the surface charge is required for bundle formation. This is a less stringent condition than that for DNA, in which case 90% of the charge needs to be neutralized for the transition to occur. The increased bundle formation by $\text{Co}(\text{NH}_3)_6^{3+}$ and polyamines compared with divalent cations is due to the higher apparent binding constants at higher valence, as predicted in the Manning theory (12).

Unique Effects of Specific Cu^{2+} Binding—Deviations from the predictions of counterion condensation reveal specific binding of cationic ligands. Bundling of F-actin by Cu^{2+} is not consistent with purely electrostatic binding. Fig. 2*a* shows the light scattering measurements after sequential additions of Cu^{2+} to 0.2 mg/ml F-actin in 150 mM KCl, without and with 20 mM MgCl_2 . For this set of experiments, we used a modified actin buffer containing 2 mM Tris at pH 7.5, 0.5 mM ATP, and 0.2 mM CaCl_2 . This change was necessary since Cu^{2+} forms insoluble precipitates with Hepes. It may also interact with dithiothreitol and NaN_3 . In the absence of MgCl_2 , large F-actin bundles start forming at 0.4 mM Cu^{2+} , a much lower value than required for other divalent cations shown in Fig. 1. This observation may be explained by specific binding of Cu^{2+} to the C terminus of actin with high affinity (28, 29), causing a reduction in the surface charge of F-actin. Although binding between Cu^{2+} and the actin C terminus is of micromolar affinity, 0.4 mM Cu^{2+} is required to form actin bundles because an additional

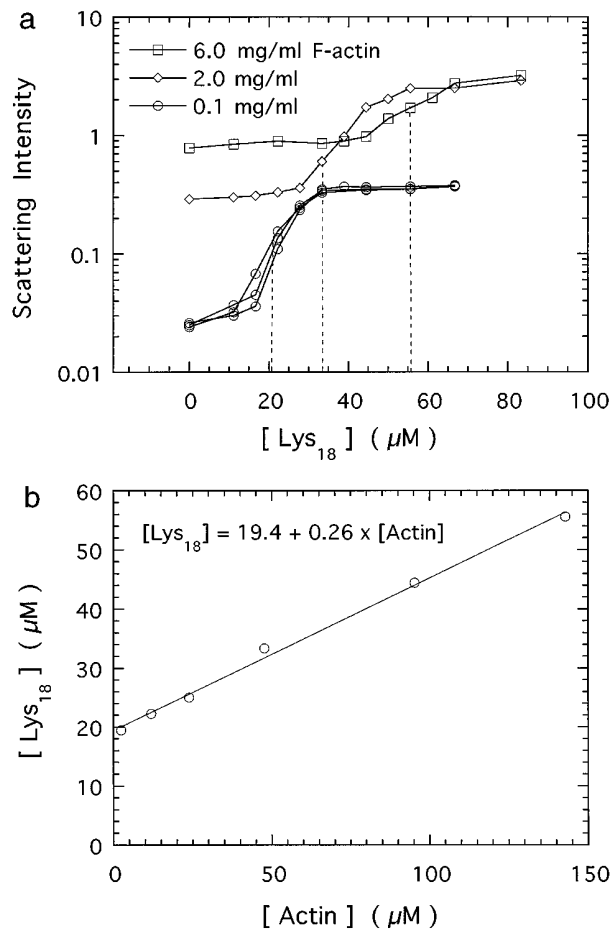


FIG. 3 Effects of F-actin concentration on the bundle formation induced by Lys_{18} . *a*, bundle formation by Lys_{18} of F-actin in 150 mM KCl at 3 representative concentrations: 0.1, 2.0, and 6.0 mg/ml. The dotted vertical lines indicate onset bundle formations determined as described in the text. *b*, the onset concentration of Lys_{18} as a function of F-actin concentration. All six experimental points were obtained as illustrated in *a*, and a linear fit was applied.

fraction of the charge must be neutralized by lower affinity interactions.

In an attempt to distinguish these two components, MgCl_2 was first added to the F-actin solution to 20 mM, in which condition the surface charge of F-actin should be neutralized to a large extent, but not enough to form bundles. A slight, yet reproducible increase in the light scattering signal was measured following addition of MgCl_2 to 20 mM, which may correspond to some other forms of aggregation, such as the fishnet-like paracrystalline structures (types I and II) characterized by a previous EM study (1). Addition of as little as 25 μM Cu^{2+} causes a significant increase in light scattering, and the high level scattering at 50 μM Cu^{2+} indicates extensive bundle formation.

A complementary set of measurements is shown in Fig. 2*b*, in which 0.2 mg/ml F-actin was first treated with various amounts of Cu^{2+} and its effect on bundling was compared with sequential addition of MgCl_2 . While 10 μM Cu^{2+} does not affect the onset of bundling by MgCl_2 , 50 μM Cu^{2+} facilitates bundle formation with only 15 mM MgCl_2 as opposed to about 30 mM required without Cu^{2+} . The decreased amount of Mg^{2+} required for bundling is due to the reduction of surface charge on F-actin caused by the tight specific binding of Cu^{2+} .

Dependence on F-actin Concentration—The amount of polyelectrolyte required to bundle different concentrations of polyelectrolyte provides information about the affinity of the interac-

tion and the degree of binding required for the bundling transition. Fig. 3a shows the increase of light scattering when actin bundling occurs with sequential addition of 18-mers of lysine Lys₁₈ to various concentrations of F-actin. The dotted lines indicate where the scattering signals increase steeply at low concentrations, or roughly double at high actin concentrations. This point is selected as the concentration of Lys₁₈ required for paracrystal formation. At high actin concentrations, the scattering intensity is relatively high prior to any bundling activity, and the increase in scattering at the onset of bundle formation is blunted by multiple scattering.

Fig. 3b shows that the amount of Lys₁₈ required to bundle actin increases approximately linearly with the actin concentration. The intercept of the vertical axis from a linear fit, $c_{18} = 19.4 \mu\text{M}$, is the concentration of free Lys₁₈ necessary to induce bundling. The slope of 0.26 Lys₁₈ per actin monomer determines the molar ratio of Lys₁₈ to actin in the bundled state. Assuming that each actin monomer carries 11 e of negative charge in the polymerized form, the number of bound polylysine per charge on the actin filament is $\theta_{18} = 0.26/11 = 0.024$. This number implies that about 40% ($\theta_{18} \times 18$) of the actin surface charge is neutralized by the lysine residues at the onset of bundling. Consistent with the Manning theory, an additional 40% or so is neutralized by the excess K⁺ to make up to 80% as the criterion for bundling to occur.

In order to explain the linear relationship measured in Fig. 3, it is helpful to first elucidate the concept of condensation zone, and how its volume is related to the molar concentration of actin. Manning introduced V_p as the volume of condensation per molar charge of the polyelectrolyte, within which counterions are bound (12). At excess univalent electrolyte, V_p can be calculated as the following,

$$V_p = 41.1 (\zeta - 1) b^3 \quad (\text{Eq. 2})$$

where V_p has the units of cm³/mol if b is expressed in Å. For F-actin, since $b = 2.5 \text{ \AA}$ and $\zeta = 7.1/b = 2.8$, we estimate V_p to be $1.2 \times 10^3 \text{ cm}^3/\text{mol}$, or equivalently 1.2 M^{-1} . The constant value for V_p implies that the total volume of condensation zone is directly proportional to the molar concentration of actin. Based on this property, a brief derivation in the appendix predicts a behavior which is consistent with Fig. 3b.

This simple exercise with the Manning theory further predicts the local ion concentration of Lys₁₈ as $c_{\text{loc}} = \theta_{18}/V_p = 0.02 \text{ M}$. The association constant, defined as the ratio of concentrations of localized to free counterions, $K = c_{\text{loc}}/c_{18}$, is therefore on the order of $20 \text{ mM}/20 \mu\text{M} = 10^3$ for the case of Lys₁₈ with 150 mM KCl in solution.

In Fig. 3b the minimal bundling concentration of Lys₁₈ is in the micromolar range, comparable to the range of F-actin concentration. In the case of divalent and trivalent cations, millimolar concentrations of free cations are required for bundle formation, and the amount sequestered by actin filaments is negligible. Measurements similar to those of Fig. 3 using Co(NH₃)₆³⁺ showed no apparent dependence of the minimal bundling concentration on actin concentration from 0.1 to 5.0 mg/ml within our experimental error of approximately 10%.

Effects of Filament Length—Although the original counterion condensation theory assumes filaments to be infinitely long, we have made no attempt to conduct our measurements with extremely long actin filament. On the contrary, small quantities (1:500 molar ratio) of gelsolin, an actin severing protein were generally added to F-actin in order to reduce the filament length to an average of 1.6 micron and thereby reduce solution viscosity (30). A systematic test of a possible length dependence for bundling of actin by polycations was made by

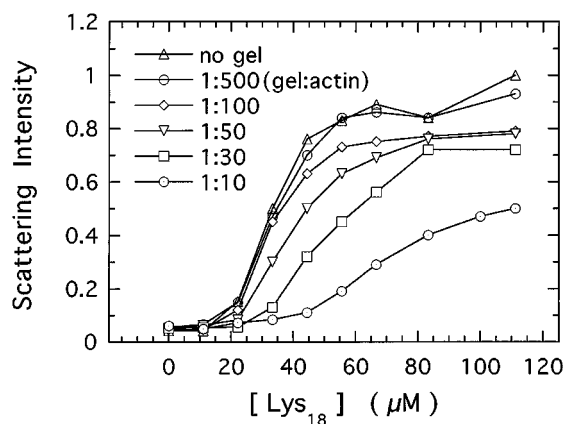


FIG. 4. Comparison of bundle formation by F-actin of various lengths. Actin concentration is 0.2 mg/ml for all the samples, with different gelsolin:actin ratios as noted in the figure. The average filament length is 1.35 μm at 1:500 molar ratio of gelsolin (*gel*) to actin.

varying the gelsolin:actin ratio. Fig. 4 shows the light scattering increases caused by adding Lys₁₈ to 0.2 mg/ml F-actin solution containing various amounts of gelsolin. The onset bundling profile varies very little until the filaments contain 50 monomers (140 nm) on average. This result implies that the basic prediction of charge condensation is applicable to cylindrical filaments of sufficiently large aspect ratios (>20:1).

Effects of Ionic Strength—A direct consequence of the Manning theory is that the association constant, K , is a function of the solution ionic strength, c , as shown below,

$$\log K = \text{constant} - N \log c \quad (\text{Eq. 3})$$

where N is the valence of the small cation. This dependence is only correct for a trace amount of polyvalent counterions in the presence of excess monovalent counterions. Otherwise, the Manning one variable approach predicts a similar power law dependence with a slope varying between 1 and N in the log-log plot, which approaches 1 with increased concentration of the polyvalent counterion. In addition, such dependence is expected to hold only at $c < 0.1 \text{ M}$. In practice, testing the ionic strength dependence for F-actin bundles is limited to high ionic strength (order of 100 mM KCl), or with 2 mM MgCl₂ in solution in order to keep actin polymerized prior to adding polycations. 0.2 mM Ca²⁺ and 0.5 mM ATP are also present in the usual buffer solutions. Nevertheless, one should still expect a marked effect of ionic strength on the minimal concentrations of polycation needed to induce bundling.

Fig. 5a displays the increasing amount of Co(NH₃)₆³⁺ required to form actin bundles in solutions of increasing KCl concentration. Fig. 5b shows the functional dependence between [Co(NH₃)₆³⁺] and [KCl]. Assuming that the concentration of Co(NH₃)₆³⁺ ions in the condensation layer reaches a fixed value of [Co(NH₃)₆³⁺]_b at the onset of bundle formation, the relation $K = [\text{Co}(\text{NH}_3)_6^{3+}]_b / [\text{Co}(\text{NH}_3)_6^{3+}]$ and the Manning theory predicts a linear dependence between $\log[\text{Co}(\text{NH}_3)_6^{3+}]$ and $\log[\text{KCl}]$ with a slope between 1 and 3. However, a linear fit to the data of Fig. 5b gives a slope of roughly 0.74. A similar experiment using Mn²⁺ instead of Co(NH₃)₆³⁺ gave a slope value as small as 0.20 (Fig. 5b). These values of less than one may be partially attributed to the complication in ionic conditions as addressed above, and to a number of oversimplified assumptions in the simplest Manning treatment. For instance, at the onset bundling condition the concentration of Co(NH₃)₆³⁺ in the condensed layer may depend on the solution ionic strength. In addition, the assumption of a charged line for F-actin is apparently oversimplified.

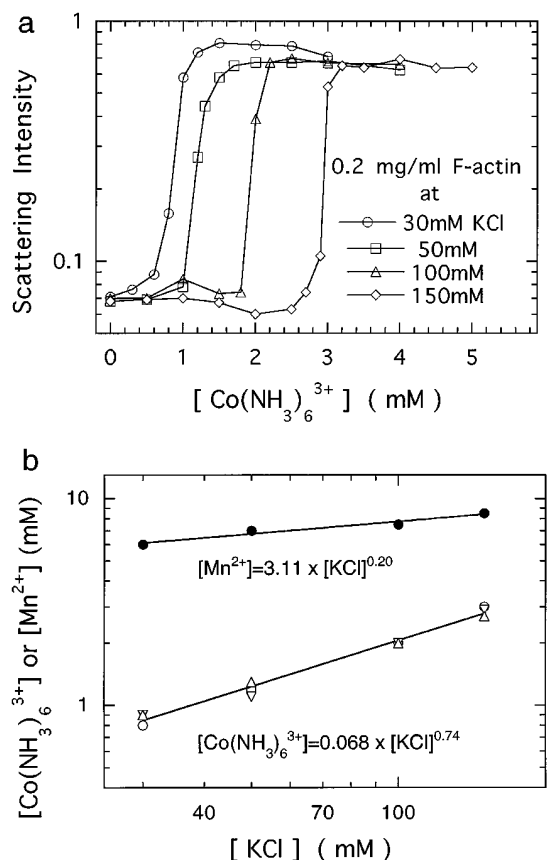


FIG. 5. **Effect of ionic strength on bundle formation.** *a*, formation of F-actin bundles by $\text{Co}(\text{NH}_3)_6^{3+}$ at four salt conditions. *b*, variation of the bundling onset concentrations of $\text{Co}(\text{NH}_3)_6^{3+}$ and Mn^{2+} versus $[\text{KCl}]$, which gives roughly the initial ionic strength. In the case of $\text{Co}(\text{NH}_3)_6^{3+}$, different types of *hollow symbols* represent measurements with actin from three independent preparations. A power law fit was applied to a total of 12 data points for $\text{Co}(\text{NH}_3)_6^{3+}$ and 4 data points for Mn^{2+} .

Nevertheless, the qualitative prediction of the polyelectrolyte treatment is confirmed.

Dissociation by Nucleotides and Other Polyanions—Addition of millimolar ATP has been reported to dissolve actin bundles formed by spermine and spermidine (4), and some actin cross-linking or bundling proteins (31–33). A very similar reversibility was found to apply to actin bundles formed by several of the polycations tested. A typical example is shown in Fig. 6*a* for actin bundles formed by Lys_{18} . Millimolar concentrations of nucleoside triphosphates such as ATP, CTP, and GTP are equally efficient in dissociating actin bundles. This reversal is consistent with competitive binding between polyanionic nucleotides and the polycations that cause actin bundling, and does not imply a specific binding of nucleotides to the actin filaments. Therefore, the process may be purely electrostatic and hence structurally nonspecific. The dependence of this effect on electrostatic charge rather than on specific structures of nucleotides is confirmed by the data of Fig. 6*b* showing that the ability to dissolve actin bundles decreases with the number of phosphates, and therefore the anionic charge, in adenine nucleotides. Di(adenosine-5')pentaphosphate and hexamers of aspartic acid dissolved the actin bundles at even lower concentrations, due to higher anionic valence (not shown).

Bundling by MARCKS Peptide—To extend the applicability of counterion effects to other agents that may function *in vivo*, experiments similar to those shown in Fig. 1 were done with the actin-binding domain of the myristoylated, alanine-rich C kinase substrate (MARCKS), a physiologically regulated actin

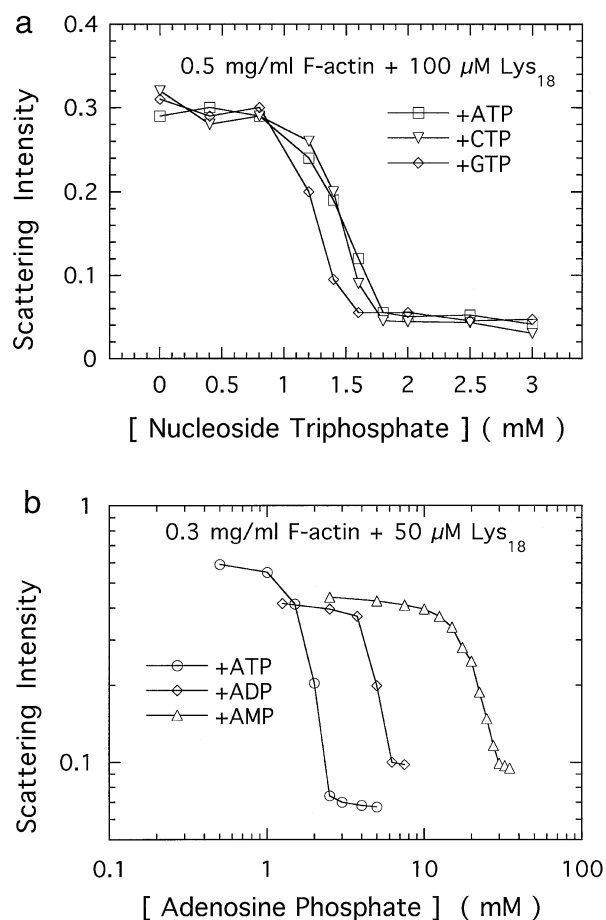


FIG. 6. **Millimolar concentrations of nucleotides reverse the formation of actin bundles.** *a*, dissociation of highly scattering bundles of 0.5 mg/ml F-actin plus 100 μM Lys_{18} following the sequential additions of ATP, CTP, and GTP, respectively. *b*, dissociation of bundles of 0.3 mg/ml F-actin plus 50 μM Lys_{18} by ATP, ADP, and AMP.

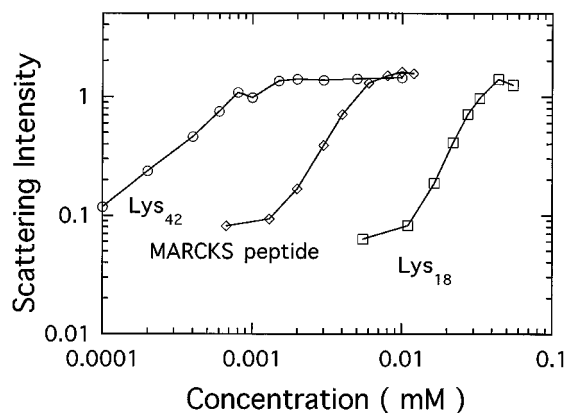


FIG. 7. **Formation of F-actin bundles induced by MARCKS peptide, in comparison with Lys_{18} and Lys_{42} .** The scattering intensity readings were roughly 0.07 for the three identical samples, prior to additions of the respective peptides.

binding protein implicated in cytoskeletal reorganization (34). A peptide based on the sequence of this domain, KKKKRFKFKSFKLSGFSFKKNNKK, bundles F-actin, and the bundling activity is lost upon phosphorylation or binding to Ca^{2+} /calmodulin (34).

Fig. 7 compares the bundling effect of MARCKS peptide with those of lysine 18-mers and 42-mers. The dose-response curves

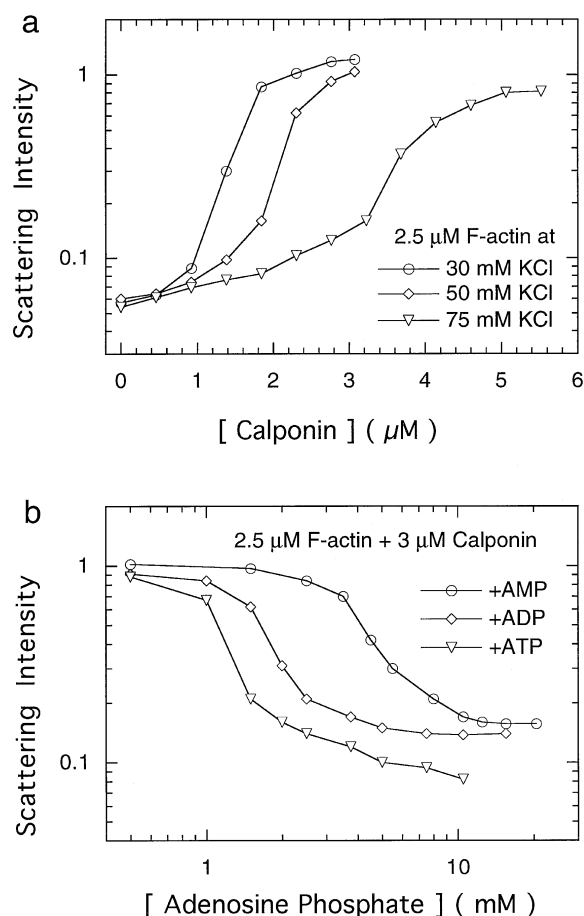


FIG. 8. **Reversible bundling activity of calponin.** *a*, effect of calponin on bundle formation by F-actin in solutions with 30, 50, and 75 mM KCl. *b*, disassembly of calponin-actin bundles by ATP, ADP, and AMP. 3 μM calponin was added to 2.5 μM F-actin with 50 mM KCl and mixed approximately 10 min prior to additions of the adenine nucleotides.

are similar, but the MARCKS peptide is effective at 1 order of magnitude lower concentration than the more highly charged Lys₁₈. In all three cases the preformed bundles dissolved after addition of millimolar ATP (not shown). It is therefore likely that the MARCKS peptide bundles actin as a consequence of its binding to the negatively charged actin surface, thereby neutralizing its electrostatic charge. In addition, cross-bridging of F-actin by long peptides may enhance bundling efficiency and possibly account for the finding that the MARCKS peptide of 14 net positive charges bundles actin more efficiently than 18-mers of lysine, since the charges on the MARCKS peptide are mainly distributed at both ends of a longer sequence. It is also possible that the MARCKS peptide self-associates into dimers or trimers and hence becomes more efficient in bundling F-actin.

Bundling by Smooth Muscle Calponin—Bundling of actin by intact proteins can also follow the predictions of counterion condensation. The smooth muscle isoform of calponin is highly basic, with roughly 8 net positive charges at neutral pH. It binds F-actin with high affinity, and the binding is reversed by phosphorylation (35). Fig. 8*a* shows the bundling of F-actin by calponin at 30, 50, and 75 mM KCl. An identical experiment with 150 mM KCl did not show a sharp increase in the light scattering at up to 6 μM calponin. These data demonstrate features qualitatively similar to those of cobalt hexamine shown in Fig. 5. Fig. 8*b* shows that the dissociation of calponin/F-actin bundles by millimolar concentrations of ATP, ADP, and

AMP is nearly identical to the dissolution of actin-lysine bundles (Fig. 6*b*). The bundling of actin by the basic isoform of smooth muscle calponin is consistent with an electrostatic mechanism like that of other polycations.

In addition to the light scattering experiments, analysis of co-sedimentation of calponin with F-actin revealed that in equimolar mixture (roughly 4 μM of each protein) the amount of calponin bound to F-actin decreased continuously with increasing ionic strength.² This result is consistent with an electrostatic model of binding, and the behavior at least partially accounts for the conflicting reports in literature of the binding stoichiometry between calponin and F-actin (32, 35–37).

DISCUSSION

Theories for counterion condensation by linear polyelectrolytes can explain the formation of actin bundles by agents as diverse as metal ions, inorganic polycations, polyamines, homopolymers of basic amino acids, peptides identified as specific actin binding sites, and intact actin binding proteins. These theories have many implications for actin structure and function, and possibly for other cytoskeletal biopolymers.

The most direct implication is that proteins with sufficient numbers of positive charges, exposed appropriately on their surface, will inevitably bind to actin filaments even in solutions of physiologic ionic strength and often with relatively high (μM) affinity. It has been noted that there are surprisingly many F-actin binding proteins, but no obvious consensus F-actin binding site has been identified (38–40). Given the strong electrostatic effects between polyelectrolytes and their counterions, the binding of some proteins to F-actin may be largely independent of unique tertiary structures that form tight specific binding interfaces typical of the protein/protein bonds that have been identified for several G-actin binding proteins. The relatively nonspecific nature of the electrostatic forces by which some proteins may bind F-actin does not necessarily mean that these interactions have no relevance *in vivo*. On the contrary, the filament density in cells is high compared to what can be achieved *in vitro*, and ionic fluxes are both common and poorly understood. The results of this work suggest that proteins that interact primarily or exclusively by electrostatic interactions can cause bundling of F-actin when present at micromolar concentrations, and such bundles can be dissolved by increasing ionic strength, protein phosphorylation, or by changes in nucleotide concentrations in the millimolar range.

The effects of polycations on F-actin show that cross-linking is not always required for bundle formation, and neutralization of sufficient surface charge on F-actin can directly induce bundling. Many actin binding domains are rich in positive charge, and long range electrostatic interaction may dominate their binding to F-actin. In this interpretation, an actin bundling protein need not contain two distinct actin binding domains, nor is dimerization required. Cross-links between parallel filaments shown in electron microscopy in some cases are perhaps merely the result of steric hindrance, and their locations are often of a stochastic nature. In the case of lateral aggregation, there is no absolute requirement for locking the filaments at the opposite sites of actin bundling proteins, although the presence of such links caused by specific actin bundling proteins, such as the acidic proteins fimbrin or villin, can modulate the structure of such bundles (39).

The analogy between bundling F-actin and DNA condensation should also be applicable to other charged biopolymers such as microtubules, intermediate filaments, filamentous bac-

² J. X. Tang, P. T. Szymanski, P. A. Janmey, and T. Tao, unpublished data.

terioophage fd, and tobacco mosaic virus. The electrostatic features such as the requirement of polycationic protein domains and the extreme sensitivity to ionic strength have been examined for lateral association of microtubules (41, 42). Parallel experiments to those reported in this paper have been extended to fd and tobacco mosaic virus suspensions (43). The nonspecific electrostatic model also explains the co-bundling of different filament types such as actin and microtubules (44), and the finding that microtubule associated proteins MAP2 and τ fragments bind and bundle F-actin (45, 46), as well as microtubules.

In addition to the formation of supermolecular aggregates, the structural dynamics of single actin filament can also be altered by the ions surrounding it, even if these ions do not have specific binding sites on the protein. Polymerization and depolymerization are extremely sensitive to the ionic conditions in solution. Many actin bundling factors accelerate actin polymerization even at lower concentrations than required for inducing the lateral aggregation of F-actin (47).

Since the condensed counterions on the surface of either F-actin or microtubules move freely along the filament axis, cells may transport metal ions such as Ca^{2+} preferentially along these filaments. This so-called cable-like property has been reported for F-actin (48), and the role of microtubules in intracellular transport may also relate to the similar polyelectrolyte nature.

Charge differences in actin subunits often occur and can accordingly alter the structure of the filament or its ability to interact with other proteins electrostatically. For example, when P_i is released from actin filament following hydrolysis of the actin-bound ATP to ADP- P_i , the surface charge density of the filament falls approximately 9% (1/11). An opposite effect would occur if actin rebound P_i or became phosphorylated. Similarly, γ and β nonmuscle actin isoforms have one or two fewer net negative charges than α -actin according to their amino acid sequence. Filaments formed by these isoforms might be more susceptible to bundling at borderline conditions, and such differences may relate to the partitioning of actin isoforms into specific structures within a cell. In a similar vein, mutations which reduce the net negative charge of actin have reportedly caused the mutant actin filaments to spontaneously bundle (49, 50). These observations provide additional evidence for the polyelectrolyte nature of F-actin and its related properties.

Applying the electrostatic model to the association between F-actin and actin binding proteins does not alter the importance of additional binding forces due to the large size and the structural variations of intact proteins. This model does not exclude the dominant effects of specific actin binding sites. Although the specific binding site may be closely related to the distribution of charged residues, the individual tertiary structures and regions of compatible hydrophobicity must also contribute to the overall association. Therefore, the sole consideration of polyelectrolyte properties of F-actin should not be exaggerated in an attempt to explain every aspect of F-actin related associations. On the other hand in those cases where tight and specific actin binding sites cannot be identified, these electrostatic interactions can lead to bindings that are remarkably efficient and regulated by physiological signals.

Acknowledgments—We thank Dr. Terrence Tao of the Boston Biomedical Research Institute for the gift of recombinant smooth muscle calponin, and Rolands Vegners for the oligomers of lysine, arginine, histidine, and aspartic acid. We also thank David J. Kwiatkowski and Thomas P. Stossel for their critical readings.

APPENDIX

We provide here a simple derivation following a chemical binding model as elucidated by Manning (12). Assuming 18-mers of lysine, Lys_{18} binds to F-actin with an apparent affinity $k = [\text{Lys}_{18}]_b / [\text{Lys}_{18}]_f$, where $[\text{Lys}_{18}]_f$ is the concentration of free lysine in solution and $[\text{Lys}_{18}]_b$ is the local concentration of lysine in the condensed region surrounding F-actin. Both k and $[\text{Lys}_{18}]_b$ are functions of the ionic strength of the excess monovalent salt and are independent of F-actin concentration.

We assume that side-by-side aggregates start to appear at a critical concentration of $[\text{Lys}_{18}]_f$. This corresponds to an undetermined, but fixed total fraction of charge neutralization of F-actin θ , which can be obtained if a Scatchard plot is provided.

In the absence of other ligands, the total concentration of oligolysine $[\text{Lys}_{18}]_o$ is an appropriate summation of $[\text{Lys}_{18}]_b$ and $[\text{Lys}_{18}]_f$ as shown in the following equation,

$$[\text{Lys}_{18}]_o = [\text{Lys}_{18}]_f + v[\text{Lys}_{18}]_b = [\text{Lys}_{18}]_f + kv[\text{Lys}_{18}]_f \quad (\text{Eq. 4})$$

where $v \ll 1$ is the volume fraction of the condensation zone surrounding F-actin in solution, and is proportional to actin concentration at a given ionic strength. Note that the volume fraction which F-actin occupies is neglected in the above expression.

Experimentally, since there is usually 0.5 mM ATP in F-actin buffer, possible formation of lysine-ATP complex should be taken into account. The complete expression based on Eq. 4 is shown below.

$$[\text{Lys}_{18}]_o = [\text{Lys}_{18}]_f + [\text{Lys}_{18}(\text{ATP})_m] + kv[\text{Lys}_{18}]_f \quad (\text{Eq. 5})$$

In the above formula, the linear dependence of $[\text{Lys}_{18}]_o$ on F-actin concentration is preserved in v , in spite of the complication due to the presence of ATP, an interacting polyion of the opposite charge.

REFERENCES

- Kawamura, M., and Maruyama, K. (1970) *J. Biochem. (Tokyo)* **68**, 885–899
- Clarke, F. M., and Morton, D. J. (1976) *Biochem. J.* **159**, 797–798
- Fowler, W. E., and Aebi, U. (1982) *J. Cell Biol.* **93**, 452–458
- Grant, N. J., Oriol-Audit, C., and Dickens, M. J. (1983) *Eur. J. Cell Biol.* **30**, 67–73
- Owen, C. H., DeRosier, D. J., and Condeelis, J. (1992) *J. Struct. Biol.* **109**, 248–254
- Stokes, D. L., and DeRosier, D. J. (1991) *Biophys. J.* **59**, 456–465
- Curmi, P. M. G., Barden, J. A., and Remedios, C. G. D. (1984) *J. Muscle Res. Cell Motil.* **5**, 423–430
- Baeza, I., Gariglio, P., Rangel, L. M., Chavez, P., Cervantes, L., Arguello, C., Wong, C., and Montanez, C. (1987) *Biochemistry* **26**, 6387–6392
- Ma, C., and Bloomfield, V. A. (1994) *Biophys. J.* **67**, 1678–1681
- Rau, D. C., Lee, B., and Parsegian, V. A. (1984) *Proc. Natl. Acad. Sci. U. S. A.* **81**, 2621–2625
- Bloomfield, V. A. (1991) *Biopolymers* **31**, 1471–1481
- Manning, G. S. (1978) *Q. Rev. Biophys.* **11**, 179–246
- Marquet, R., and Houssier, C. (1991) *J. Biomol. Struct. Dynam.* **9**, 159–167
- Ray, J., and Manning, G. S. (1994) *Langmuir* **10**, 2450–2461
- Oosawa, F. (1971) *Polyelectrolytes*, pp. 120–126, Marcel Dekker, Inc., New York
- Delville, A., Galboa, H., and Laszlo, P. (1982) *J. Chem. Phys.* **77**, 2045
- Delville, A., and Laszlo, P. (1983) *Biophys. Chem.* **17**, 119
- Le Bret, M., and Zimm, B. H. (1984) *Biopolymers* **23**, 287–312
- Schmitz, K. S. (1993) *Macroions in Solution and Colloidal Suspension*, pp. 213–268, VCH, New York
- Sanchez-Sanchez, J. E., and Lozada-Cassou, M. (1992) *Chem. Phys. Lett.* **190**, 202–208
- Le Bret, M., and Zimm, B. H. (1984) *Biopolymers* **23**, 271–285
- Dewey, T. G. (1990) *Biopolymers* **29**, 1793–1799
- Sharp, K. A., Friedman, R. A., Misra, V., Hecht, J., and Honig, B. (1995) *Biopolymers* **36**, 245–262
- Sheterline, P., and Sparrow, J. (1994) *Protein Profile* **1**, 1–121
- Spudich, J., and Watt, S. (1971) *J. Biol. Chem.* **246**, 4866–4871
- Kurokawa, H., Fujii, W., Ohmi, K., Sakurai, T., and Nonomura, Y. (1990) *Biochem. Biophys. Res. Commun.* **168**, 451–457
- Stafford, W. F., III, Mabuchi, K., Takahashi, K., and Tao, T. (1995) *J. Biol. Chem.* **270**, 10576–10579
- Lehrer, S. S., Nagy, B., and Gergely, J. (1972) *Arch. Biochem. Biophys.* **150**, 164–174
- Drabikowski, W., Lehrer, S., Nagy, B., and Gergely, J. (1977) *Arch. Biochem. Biophys.* **181**, 359–361
- Janmey, P. A., and Käs, J. (1994) in *Annual Transactions of the Nordic*

- Rheology Society* (Saasen, A., ed) pp. 8–11, HCO Tryk, Copenhagen
31. Albanesi, J. P., Lynch, T. J., Fujisaki, H., Bowers, B., and Korn, E. D. (1987) *J. Biol. Chem.* **262**, 3404–3408
 32. Kolakowski, J., Makuch, R., Stepkowski, D., and Dabrowska, R. (1995) *Biochem. J.* **306**, 199–204
 33. Okagaki, T., and Asakura, S. (1987) *J. Biochem. (Tokyo)* **101**, 189–197
 34. Hartwig, J. H., Thelen, M., Rosen, A., Janmey, P. A., Nairn, A. C., and Aderem, A. (1992) *Nature* **356**, 618–622
 35. Winder, S. J., and Walsh, M. P. (1990) *J. Biol. Chem.* **265**, 10148–10155
 36. Lu, F. W. M., Freedman, M. V., and Chalovich, J. M. (1995) *Biochemistry* **34**, 11864–11871
 37. Makuch, R., Birukov, K., Shirinsky, V., and Dabrowska, R. (1991) *Biochem. J.* **280**, 33–38
 38. Matsudaira, P. (1991) *Trends Biochem. Sci.* **16**, 87–92
 39. Otto, J. J. (1994) *Curr. Opin. Cell Biol.* **6**, 105–109
 40. Stossel, T. P., Chaponnier, C., Ezzell, R. M., Hartwig, J. H., Janmey, P. A., Kwiatkowski, D. J., Lind, S. E., Smith, D. B., Southwick, F. S., Yin, H. L., and Zaner, K. S. (1985) *Annu. Rev. Cell Biol.* **1**, 353–402
 41. Pedrotti, B., Colombo, R., and Islam, K. (1994) *Biochemistry* **33**, 8798–8806
 42. Pedrotti, B., and Islam, K. (1994) *Biochemistry* **33**, 12463–12470
 43. Tang, J. X., Wong, S., Tran, P. T., and Janmey, P. A. (1996) *Berichte der BunsenGesellschaft: Proceeding of Polyelectrolytes, Potsdam, Germany, Sep. 18–22, 1995*, VCH, Weinheim
 44. Itano, N., and Hatano, S. (1991) *Cell Motil. Cytoskel.* **19**, 244–254
 45. Selden, S. C., and Pollard, T. D. (1983) *J. Biol. Chem.* **258**, 7064–7071
 46. Yamauchi, P. S., and Purich, D. L. (1993) *Biochem. Biophys. Res. Commun.* **190**, 710–715
 47. Oriol-Audit, C., Hosseini, M. W., and Lehn, J. (1985) *Eur. J. Biochem.* **151**, 557–559
 48. Lin, E. C., and Cantiello, H. F. (1993) *Biophys. J.* **65**, 1371–1378
 49. Johara, M., Toyoshima, Y. Y., Ishijima, A., Kojima, H., and Yanagida, T. (1993) *Proc. Natl. Acad. Sci. U. S. A.* **90**, 2127–2131
 50. Cook, R. K., Blake, W. T., and Rubenstein, P. A. (1992) *J. Biol. Chem.* **267**, 9430–9436
 51. Gong, B. J., Mabuchi, K., Takahashi, K., Nadal-Ginard, B., and Tao, T. (1993) *J. Biochem. (Tokyo)* **114**, 453–456